ARTICLE
Journal of Cellular Biochemistry 112:2266–2278 (2011)

Journal of Cellular Biochemistry

Isolation and Characterization of Squamous Carcinoma Cells Resistant to Photodynamic Therapy

Laura N. Milla,[1*] Ingrid S. Cogno,[1] Matías E. Rodríguez,[1] Francisco Sanz-Rodríguez,[2] Alicia Zamarrón,[2] Yolanda Gilaberte,[3] Elisa Carrasco,[2] Viviana A. Rivarola[1] and Ángeles Juarranz[2**]

[1]*Departamento de Biología Molecular, Facultad de Ciencias Exactas, Físico-Químicas y Naturales, Universidad Nacional de Río Cuarto, Río Cuarto 5800, Córdoba, Argentine*

[2]*Departamento de Biología, Facultad de Ciencias, Universidad Autónoma de Madrid, Cantoblanco 28049, Madrid, Spain*

[3]*Servicio de Dermatología, Hospital San Jorge, Huesca, Spain*

ABSTRACT

Photodynamic therapy (PDT) employing methyl δ-aminolevulinic acid (Me-ALA), as a precursor of the photosensitizer protoporphyrin IX (PpIX), is used for the treatment of non melanoma cutaneous cancer (NMCC). However, one of the problems of PDT is the apparition of resistant cell populations. The aim of this study was to isolate and characterize squamous carcinoma cells SCC-13 resistant to PDT with Me-ALA. The SCC-13 parental population was submitted to successive cycles of Me-ALA-PDT and 10 resistant populations were finally obtained. In parental and resistant cells there were analyzed the cell morphology (toluidine blue), the intracellular PpIX content (flow cytometry) and its localization (fluorescence microscopy), the capacity of closing wounds (scratch wound assay), the expression of cell-cell adhesion proteins (E-cadherin and β-catenin), cell-substrate adhesion proteins (β1-integrin, vinculin and phospho-FAK), cytoskeleton proteins (α-tubulin and F-actin) and the inhibitor of apoptosis protein survivin, in the activated form as phospho-survivin (indirect immunofluorescence and Western blot). The results obtained indicate that resistant cells showed a more fibroblastic morphology, few differences in intracellular content of the photosensitizer, higher capacity of closing wounds, higher number of stress fibers, more expression of cell-substrate adhesion proteins and higher expression of phospho-survivin than parental cells. These distinctive features of the resistant cells can provide decisive information to enhance the efficacy of Me-ALA applications in clinic dermatology. J. Cell. Biochem. 112: 2266–2278, 2011.

KEY WORDS: CUTANEOUS CANCER; METHYL-Δ-AMINOLEVULINIC ACID; PHOTODYNAMIC THERAPY; RESISTANCE

It is estimated that cutaneous tumors represent a 33.33% of all human cancers. NMCC is the most frequently skin cancer representing 90–95% of the cutaneous cancers. NMCC include basal cell carcinoma (BCC) and squamous cell carcinoma (SCC) [Ricotti et al., 2009]. Photodynamic therapy (PDT) is widely employed for treatment of NMCC [Szeimies et al., 2005]. PDT consists in the administration of a photosensitizing drug followed of its activation with visible light. This activation produces formation of oxygen reactive species, mainly singlet oxygen, that cause tumor cells death [Dougherty et al., 1998].

In the last years, there were developed new compounds with PDT applications, including δ-aminolevulinic acid (ALA), a precursor

Abbreviations: ALA, δ-aminolevulinic acid; BCC, basal cell carcinoma; CAM, cell adhesion molecules; IAP, inhibitor of apoptosis protein; Me-ALA, methyl δ-aminolevulinic acid; NMCC, no melanoma cutaneous cancer; PDT, photodynamic therapy; PpIX, protoporphyrin IX; SCC, squamous cell carcinoma.

Ingrid Sol Cogno and Matías Exequiel Rodríguez contributed equally to this work.

Grant sponsor: Agencia Española de Cooperación Internacional; Grant number: AECI, A/010492/07; Grant sponsor: Consejo Nacional de Investigación Científica y Tecnológica (CONICET); Grant sponsor: Secretaría de Ciencia y Técnica (SeCyT), Universidad Nacional de Río Cuarto (UNRC); Grant sponsor: PICT Agencia FONCYT; Grant sponsor: Ministerio de Ciencia e Innovación, Spain; Grant number: FIS, PS09/0199.

*Correspondence to: Laura Milla Sanabria, Rute 8 and 36 km 601, Universidad Nacional de Río Cuarto, Río Cuarto (5800), Córdoba, Argentine. E-mail: lmilla@exa.unrc.edu.ar

**Correspondence to: Ángeles Juarranz, Darwin 2, Universidad Autónoma de Madrid, Cantoblanco (28049), Madrid, Spain. E-mail: angeles.juarranz@uam.es

Received 13 November 2010; Accepted 5 April 2011 • DOI 10.1002/jcb.23145 • © 2011 Wiley-Liss, Inc.

Published online 18 April 2011 in Wiley Online Library (wileyonlinelibrary.com).

metabolite of the photoactive compound PpIX intermediary in the synthesis of hemo group [Josefsen and Boyle, 2008]. Currently, hydrocarbonated esters derivatives of ALA, such as the methyl ester derivative Me-ALA are employed. Methyl derivative Metvix® (Photocure ASA, Noruega) is approved in Europe, Australia, New Zealand and Brazil for keratosis actinic (a precancerous cutaneous lesion) and superficial and nodular BCCs treatment [Szeimies, 2007].

One of the problems of PDT [Sieró et al., 2004] and other anticancer therapies is the apparition of resistant cell populations [Perona and Sánchez-Pérez, 2004]. These cells would be responsible of relapses and metastatic processes. The incapacity to suffer apoptosis in response to treatment consents a selective advantage in the tumor progression and resistance to therapies [Kitano, 2007]. In the tumor cells there are numerous mechanisms of resistance [Hazlehurst et al., 2003; Solyanik, 2010]. There was reported that the inhibitor of apoptosis protein of the IAPs family, called survivin, is over-expressed in tumor cells and it is related with chemo and radio-resistance [Zaffaroni et al., 2002; Rodel et al., 2005]. Also, resistance mechanisms that are recently being described are mediated by cell adhesion molecules (CAM), such as the cell-cell adhesion proteins that constitute the adherent junctions (E-cadherin, α-catenin and β-catenin) and cell-substrate adhesion proteins that form part of focal adhesions (integrins, vinculin, FAK, among others) [Seidler et al., 2005; Hehlgans et al., 2007]. Integrins mediate interactions of the actin cytoskeleton with extracellular matrix. β1-integrins are well known to confer resistance to clinically administered chemotherapeutic drugs or ionizing radiation [Cordes and Meineke, 2003; Estrugo et al., 2007], given that these induce the activation of a survival regulating cascade via PI3K/Akt [Velling et al., 2004] and inhibit caspase 8 activation [Estrugo et al., 2007]. Alterations in the cell adhesion caused by PDT have been previously described for several authors [Rousset et al., 1999; Uzdensky et al., 2004; Buytaert et al., 2007; Casas et al., 2008], although the implication of this event in tumor resistance remains to be elucidated.

The objective of this work was to isolate and characterize squamous carcinoma cells SCC-13 resistant to repeated photodynamic treatments with methyl δ-aminolevulinic acid. The particular characteristics of the resistant cells could provide decisive information that facilitate to understand and predict the action of PpIX precursors and to enhance the efficacy of Me-ALA applications in clinic dermatology.

MATERIALS AND METHODS

PHOTOSENSITIZER

The compound used in this study was the methyl derivative of δ-aminolevulinic acid (Sigma-Aldrich, St. Louis, MO). A stock solution of 10 mM Me-ALA was prepared in deionized sterile water from which 1 mM work solution was made employing DMEM culture medium without serum.

ANTIBODIES

The primary antibodies employed were: anti-rabbit monoclonal antibody against survivin (Cell signaling Technology, Inc. Danvers, MA), anti-rabbit policlonal antibody against phospho-survivin (Santa Cruz Biotechnology, Santa Cruz, CA), anti-mouse monoclonal antibodies against E-cadherin, β-catenin, FAK, phospho-FAK, β1-integrin (BD Transduction Laboratories), β-catenin active (Millipore, Co., MA), vinculin and α-tubulin (Sigma-Aldrich. St. Louis, MO). The secondary antibodies used were: HRP monoclonal antibody anti-Ig G of mouse and HRP monoclonal antibody anti-Ig G of rabbit (Amersham Pharmacia Biotech, Little Chalfont, UK), monoclonal antibodies anti-Ig G of mouse and rabbit FITC-labeled (Sigma-Aldrich. St. Louis, MO).

CELL LINE AND CELL CULTURE

This study was made employing the cancer human cell line of squamous cell carcinoma SCC-13 [Rheinwald and Beckett, 1981]. SCC-13 cells were cultured in complete medium DMEM (Dulbecco's modified Eagle medium high glucose 1X, Gibco Invitrogen corp., Carlsbad, CA) supply with 10% fetal bovine serum (PAA Laboratories GmbH, Pasching, Austria) 1% of glutamine (GlutaMAX™ 100X, Gibco Invitrogen corp., Carlsbad, CA), 1% antibiotic (Penicillin 10,000 units/mL−streptomycin 10,000 μg/mL, Gibco Invitrogen corp., Carlsbad, CA) and 0.5% of sodium pyruvate 100 mM (Gibco Invitrogen corp., Carlsbad, CA). Cells were incubated at 37°C in an atmosphere containing 5% CO_2.

INDUCTION OF RESISTANCE TO Me-ALA-PDT

SCC-13 cells were cultured in 25 cm^2 flasks and incubated with Me-ALA 1 mM for 4 h. Thereafter, cells were exposed to different light doses of red light (635 nm ± 17 nm; 7–25 J/cm^2). Treatment conditions that caused survival rates of 5–10% were chosen. The surviving cells were harvested at 24 h after PDT and replated. When cells proliferated, they were submitted to a new PDT treatment [Luna and Gomer, 1991]. The final population received a total of 10 cycles of PDT. The initial population, not subjected to PDT, was called parental population, the cellular population submitted to one PDT treatment was called first resistant generation and so the following generations were named consecutively. When resistant cells were obtained they were maintained in frozen stocks. At least three different cultures were obtained for each generation (1st to10th) checking their resistance abilities by the MTT assay after PDT treatment. For the experiments parental and resistant cells were used until 7 passages. Parental, 5th and 10th resistance cell generations were selected for the studies. Also, for MTT and Western Blot analysis 1st generation was included.

MTT ASSAY

Cell viability was analyzed by the MTT (3-[4,5-dimethylthiazol-2-yl]-2,5-diphenyltetrazoliumbromide) assay, a method based on the activity of mitochondrial dehydrogenases. The cells were incubated with Me-ALA 1 mM for 4 h at 37° and then irradiated at 7.31 J/cm^2 ($n = 8$). Cells without drug neither light were employed as controls ($n = 8$) and they were expressed as 100% of viability. Cells with drug, but without light were employed as drug controls ($n = 8$); cells with light at 7.31 J/cm^2, but without drug were employed as light controls ($n = 8$). After 24 h of treatments, cells were incubated with MTT (1 mg MTT:1 ml PBS:9 ml DMEM 10% serum) for 1 h and formazan crystals were suspended in DMSO. Measures of the absorbance were taken at 540 nm. The experiment was performed three times. The quantification of the results was made from a representative experiment.

LIGHT SOURCE

Cells were irradiated employing a monochromatic light source (635 nm ± 17 nm) with a multi-LED system (coherent light) at irradiation intensity of 1.65 mW/cm^2 (as measured by Coherent Lasermate power meter).

CELL MORPHOLOGY AND NUCLEAR MORPHOLOGY

In order to analyze the cell morphology, cells cultured over coverslips were fixed in methanol and stained with toluidine blue (0.05% w/v in distilled water) (Merck Biosciences, La Jolla, CA). After washing and air drying, preparations were mounted in DePeX (SERVA Electrophoresis GmbH, Heidelberg, Germany). This experiment was performed three times.

For nuclear staining, cells were fixed in formaldehyde (3.7% v/v formaldehyde/PBS, 4°C), stained with 2.5 μg/ml Höechst (H-33258, Sigma-Aldrich, St. Louis, MO) and mounted in ProLong (Invitrogen, San Diego, CA). Giant nucleuses were determinated as those with 20 μM or more of diameter. To determinate the percentage of giant nucleuses or micronuclei a total of 1,000 cells were observed and the count was realized on three different samples.

MEASUREMENT OF INTRACELLULAR PpIX

When cells cultivated in P6 plaques reached a confluence of 70% they were incubated with Me-ALA 1 mM for 1 and 4 h at 37°C. Cells without drug were employed as controls. Afterward, cells were tripsinized, centrifugated for 10 min at 2,000 rpm, resuspended and fixed with 3.7% v/v formaldehyde/PBS for 15 min at 25°C. The cell suspensions were again centrifugated (5 min, 2,000 rpm) and then resuspended in PBS. The PpIX emission measures were collected employing a flow cytometer Cytomics FC500 (Beckman Coulter, USA) ($\lambda_{exc} = 625$ nm; $\lambda_{em} = 670$ nm). The fluorescence intensity was determinated from 10,000 cells for each cellular population and this assay was performed three times.

SUBCELLULAR LOCALIZATION OF PpIX

When cells cultivated on coverslips reached a confluence of 70% they were incubated with Me-ALA 1 mM for 4 and 17 h at 37°C. Then, cells were washed with PBS, mounted on slides and observed in situ under the fluorescence microscope using an exciting light of 460 nm. The subcellular PpIX localization was analyzed comparing the fluorescent signal emitted by PpIX with that obtained by fluorescent markers of selective subcellular accumulation: Mitotracker Green (Invitrogen, San Diego, CA) to mitochondria, Acridine Orange (Invitrogen, San Diego, CA) and Lisotracker Green (Invitrogen, San Diego, CA) to lisosomes and NBD C6-ceramide (Invitrogen, San Diego, CA) to Golgi apparatus. The markers were applied to the cells following the instructions of the commercial procedures. We also analyzed the colocalization of PpIX ($\lambda_{exc} = 460$–90 nm) with Mitotracker or Lisotracker Green ($\lambda_{exc} = 545$–80 nm). Cells were incubated with Me-ALA 1 mM for 17 h, the medium containing Me-ALA was discarded and further the cells were incubated for 15 min with medium containing Mitotracker or Lisotracker Green 0.1 μM according to commercial procedures. This assay was performed two times.

SCRATCH WOUND ASSAY

SCC parental cells 5th and 10th generations were cultivated in multi-wells P12 with complete medium. When cells reached a confluence of 95%, wounds were made in the cell culture using a tip. Photographs were taken at 0, 4, 8, 12, and 24 h, after wounds were produced (n = 8). The wound widths were measured employing Image Pro-Plus 6. The experiment was performed three times. The quantification of the results was made from a representative experiment.

INDIRECT IMMUNOFLUORESCENCE

For inmunodetection of α-tubulin, cells raised on coverslips were fixed in cold methanol (−20°C) for 10 min, then were fixed in acetone for 1 min and were rehydrated in graded ethanol-PBS solutions. In the case of E-cadherin, β-catenin, vinculin, phospho-FAK and phospho-survivin detection, cells were fixed in 4% formaldehyde (4°C) for 30 min and permeated with 0.1% triton X-100 in PBS (v/v) for 10 min. Cells were incubated with the first antibodies (dilution 1:50) for 1 h at 37°C, washed in PBS, incubated with FITC-labeled secondary antibody (dilution 1:200) for 1 h at 37°C and finally washed in PBS.

F-actin microfilaments were marked with phalloidin-rhodamin. Cells were fixed in 4% formaldehyde for 30 min and permeated with 0.1% triton X-100 in PBS (v/v) for 10 min. Then, cells were incubated with phaloidin-rhodamin for 30 min at 25°C and washed in PBS.

All the preparations were counterstained with 2.5 μg/ml H-33258 (Sigma-Aldrich. St. Louis, MO) for 2 min, washed in PBS and finally mounted in ProLong (Invitrogen, San Diego, CA). This assay was performed two times for each protein. Microscopic observation was realized in a fluorescence microscope Olympus BX61. Photographs were taken employing a digital camera Olympus DP50.

IMAGE PROCESSING

To evaluate differences in the organization pattern of F-actin cytoskeleton networks [Buño et al., 1998], regions with a representative and comparable distribution of cells were subjected to image processing using the public domain ImageJ 1.37v software (http://rsb.info.nih.gov/ij/). Convolved images were obtained by means of the corresponding filter (a matrix of 25 points (5 columns and 5 rows), the central point with a +25 value and the remaining peripheral points with a 1 value).

WESTERN BLOTS

SCC cells of parental population and resistant cells of first, fifth, and tenth generations were lysed in triton buffer (50 mM Tris-HCl pH 7.4, 100 mM NaCl, 5 mM $MgCl_2$, 5 mM $CaCl_2$, 1% Igepal, 1% triton X-100). The suspensions were centrifuged at 13,000 rpm for 5 min. The supernatants containing cytoplasmatic and membrane proteins were collected for detection of E-cadherin, β-catenin, FAK, phospho-FAK, β1-integrin, vinculin and α-tubulin. For immunoblot of survivin and phospho-survivin, cells were lysed with RIPA buffer (150 mM NaCl, 1% Triton X-100, 1% deoxycholate, 0.1% SDS, 10 mM Tris-HCl pH 7.2, 5 mM EDTA, Phosphatase Cocktail and Protease Inhibitor Cocktail (Sigma-Aldrich, St. Louis, MO)). Proteins concentration was measured by BCA™ Protein Assay Kit (Thermo Scientific Pierce, Rockford, IL). The proteins were electrophoresed and blotted on Immobilon-P PVDF membranes (Millipore Co., MA).

Membranes were blocked in PBS-tween 0.1% with 5% non-fat dried milk for 1 h at 25°C and then incubated with the first antibody overnight at 4°C. After washing with PBS-tween 0.1%, membranes were subjected to the peroxidase-conjugated secondary antibody and developed by chemiluminescence (ECL, Amersham Pharmacia Biotech, Little Chalfont, UK). This assay was performed three times for each protein.

STATISTICAL TREATMENT

The values in the figures and table are expressed as mean ± standard errors. ANOVA test was used to determinate statistical differences among means in the MTT and the scratch wound assays. $P < 0.05$ are considered significant (Infostat).

RESULTS

INDUCTION OF RESISTANCE TO ME-ALA-PDT

With the objective of obtaining SCC-13 resistant cell populations, cells were incubated with Me-ALA 1 mM for 4 h. Then, cells were exposed to red light along variable times. Treatment conditions that caused survival rates of 5–10% were chosen. Figure 1A show the irradiation doses employed to obtain the SCC PDT-resistant generations. Stronger irradiation conditions were necessary to get the last resistant generations. To obtain the 1st and 2nd SCC-13 generations, cells were irradiated at a light dose of 7.31 J/cm^2. Then, to obtain the 3rd and 4th generations the necessary irradiation was 11.33 J/cm^2; 14.99 J/cm^2 for 5th, 6th, and 7th generations; 24.78 J/cm^2 to obtain 8th and 9th generations and to obtain the 10th generation it was necessary a light dose of 25 J/cm^2. We further studied biological characteristics of 5th and 10th resistant populations comparing to SCC-13 parental cells.

To measure the resistant grade of the cells the viability after PDT was measured in parental cells, 1st, 5th, and 10th generations. When cells were subjected to PDT, with Me-ALA 1 mM and irradiation of 7.31 J/cm^2, parental and 1st generation cells had a viability of 10%, while 5th generation has 85% and 10th generation has 95% of viability, with statistic differences for both resistant generation respect to parental ($P < 0.01$) (Fig. 1B).

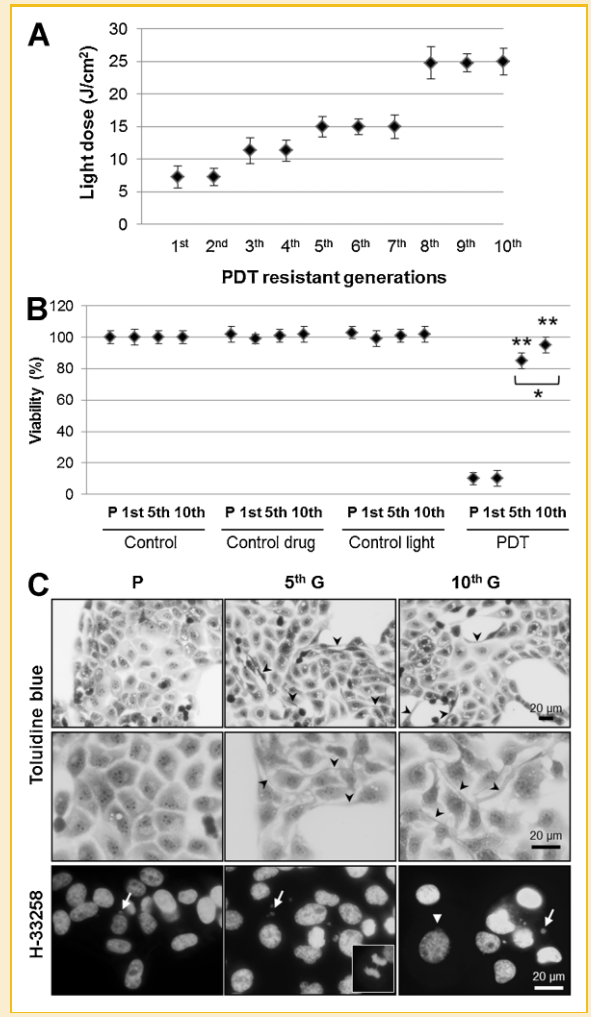

Fig. 1. SCC-13 PDT-resistant cells. A: Light doses in J/cm^2 necessary to obtain the different generations of SCC-13 PDT-resistant cells. Treatment conditions that caused survival rates of 5–10% were chosen. Me-ALA 1 mM was incubated for 4 h and thereafter, cells were subjected to red light irradiation (635 nm ± 17 nm). The values represent means ± standard errors. n = 3. B: Cell viability of SCC-13 parental, 1st, 5th, and 10th generations by MTT assay after PDT. Me-ALA 1 mM was incubated for 4 h and cells were irradiated at 7.31 J/cm^2. The values represent means ± standard errors. n = 8. * $P < 0.05$ (5th G-PDT h vs 10th G-PDT). ** $P < 0.01$ (5th G-PDT vs P-PDT; 10th G-PDT vs P-PDT). C: Cell morphology through toluidine blue and Höechst (H33258) staining of SCC-13 parental, 5th and 10th PDT resistant generations. Notice the presence of fibroblastic projections (black arrow heads), giant nucleuses (white arrow head) and micronuclei (white arrows) in 5th and 10th generations. The insert in 5th G shows an anaphase in which some chromosomes do not migrate to the poles. G: generation. P: parental. Scale bar: 20 μm.

CELL MORPHOLOGY AND NUCLEAR MORPHOLOGY

The general morphology of SCC-13, parental and resistant generations was analyzed after toluidine blue staining. Parental SCC-13 cells showed diverse morphology, from poliedric to fibroblastic with long prolongations (Fig. 1C). These morphologies were also observed in the 5th and 10th isolated generations; although these populations had a higher proportion of fibroblastic forms (black head arrows) and the cell colonies were more expansive with respect to the SCC parental populations.

Nuclear morphology analyzed after staining with H-33258 revealed that rounded and oval nucleuses, among other forms, were presented in the three SCC-13 populations studied (Fig. 1C). Also, long nuclear connections were found between two nucleuses of two cells than divided. Giant nucleuses (polyploidy) were observed in higher proportion in resistant cells of 5th (1.2 ± 0.35%) and 10th (2.1 ± 0.4%) generations than parental cells (0.5 ± 0.2%) (arrow white head). In addition, it was observed an increase in the number of cells with micronuclei (white arrows) in 5th (6 ± 1.3%) and 10th (12% ± 2.8) generations comparing to parental SCC-13 cells (3 ± 1.3%). In general, normal cell divisions were observed; however, cells in abnormal anaphase or telophase with chromosomal material that stayed in the middle of the two poles were also found mainly in 5th and 10th generation (Fig. 1C, insert).

MEASUREMENT OF INTRACELLULAR PpIX

Since the amount of intracellular PpIX might affect the phototoxicity, we examined if the differential cytotoxicity was due to the different PpIX content in parental and resistant cells. The production of PpIX by the three populations of SCC-13 cells was determined by flow citometry ($\lambda_{exc} = 625$ nm) after 1 and 4 h of incubation with Me-ALA. In control cells (without Me-ALA incubation) PpIX was not detected. As it can be seen in the Figure 2 and the Table I, there were not differences in the PpIX fluorescence intensity between resistant and parental cells after 1 h of Me-ALA incubation. At 4 h after drug incubation lower fluorescence intensity of the photosensitizer was found in resistant cells of 5th (0.90 ± 0.16 arbitrary units, AU) and 10th generation (1.18 ± 0.27 AU) in respect to parental cells (1.83 ± 0.16 AU).

SUBCELLULAR LOCALIZATION OF PpIX

In order to determine PpIX localization, SCC-13 parental cells, 5th and 10th generations were observed in the fluorescence microscope after 4 and 17 h of Me-ALA 1 mM incubation. Under 460–490 nm excitation light, PpIX was fluoresced in red. At 4 h of Me-ALA incubation, PpIX was localized in the plasmatic membrane in all analyzed populations (Fig. 3A); but very low fluorescence intensity was also detected into lysosomes and mitochondrias and in cytoplasm. At 17 h of incubation, PpIX was clearly detected in plasmatic membrane, lysosomes, mitochondrias, and cytoplasm in all analyzed populations, being the red fluorescence intensity much higher compared with that of 4 h of incubation. In addition, PpIX was observed in vacuoles, especially in the 5th cell population (arrows in Fig. 3A). The Figure 3B shows the colocalization of PpIX with Mitotracker Green (MTG) or Lisotracker Green (LTG) in parental cells at 17 h of Me-ALA incubation; this colocalization was also found in 5th and 10th generations.

The differences in the PpIX fluorescence intensity founded by flow citometry at 4 h of Me-ALA incubation between parental and 5th generation can not be detected by fluorescence microscopy due the immediate photoblenching of the PpIX under the microscopy exciting light of 460–490 nm.

CELL MIGRATION BY SCRATCH WOUND ASSAY

We examined the ability of migration and of closing wounds by scratch wound assay at 4, 8, 12 and 24 h after wounds were done in SCC-13 parental and in the PDT-derived variants 5th and 10th resistant generations. The migration capacity must been analyzed before the cells suffer divisions. At 4 and 8 h after the wounds are open, all the three populations do not divide, therefore we studied the migration at these hours. When cells begin to divide we can analyze the capacity of closing wounds because of cell proliferation.

TABLE I. Analysis of PpIX Through Flow Cytometry in SCC-13 Parental and Resistant Cells Exposed to Me-ALA

	P	5th	10th
1 h	0.55 ± 0.07	0.54 ± 0.11	0.61 ± 0.04
4 h	1.83 ± 0.36	0.90 ± 0.16	1.18 ± 0.27

PpIX fluorescence intensity (AU) after 1 and 4 h 1 mM Me-ALA incubation. Mean ± SD; n = 3; number of events: 10,000.

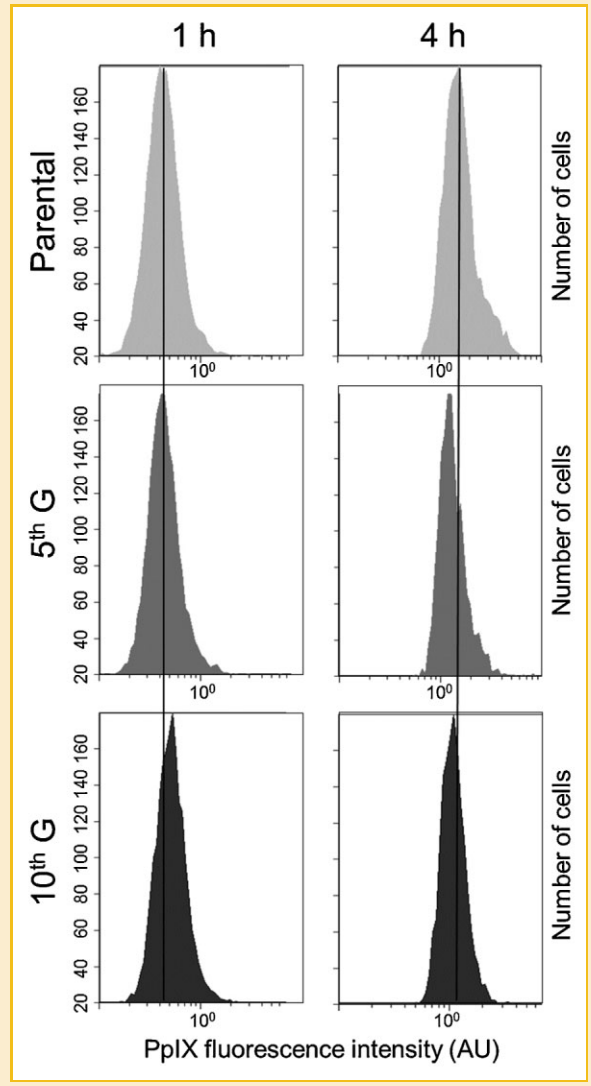

Fig. 2. PpIX fluorescence intensity (AU = arbitrary units) through flow cytometry. SCC-13 parental, 5th and 10th PDT resistant generations were incubated with Me-ALA 1 mM for 1 and 4 h. n = 3; number of events: 10,000. G: generation. P: parental.

After 8 h and before the 12 h, all the three SCC-13 populations begin to suffer divisions, for that reason we analyzed the capacity of closing wound because of cell proliferation at 12 and 24 h.

As it is observed in Figure 4A and B, differences in the migration capacity between resistant and parental cells were not found at 4 and 8 h after the assay was started. However, resistant cells showed higher capacity of closing wounds, because at 12 and 24 h the scratches were narrower in 5th ($P < 0.05$ to 12 and 24 h) and 10th ($P < 0.01$ to 12 h and $P < 0.05$ to 24 h) generations compared with parental cells.

CELL–CELL ADHESION PROTEINS

The expression of cell-cell adhesion proteins that constitute the adherent junctions were analyzed through indirect immunofluorescence and Western blot. There were not differences in the expression patterns and levels of E-cadherin and β-catenin between

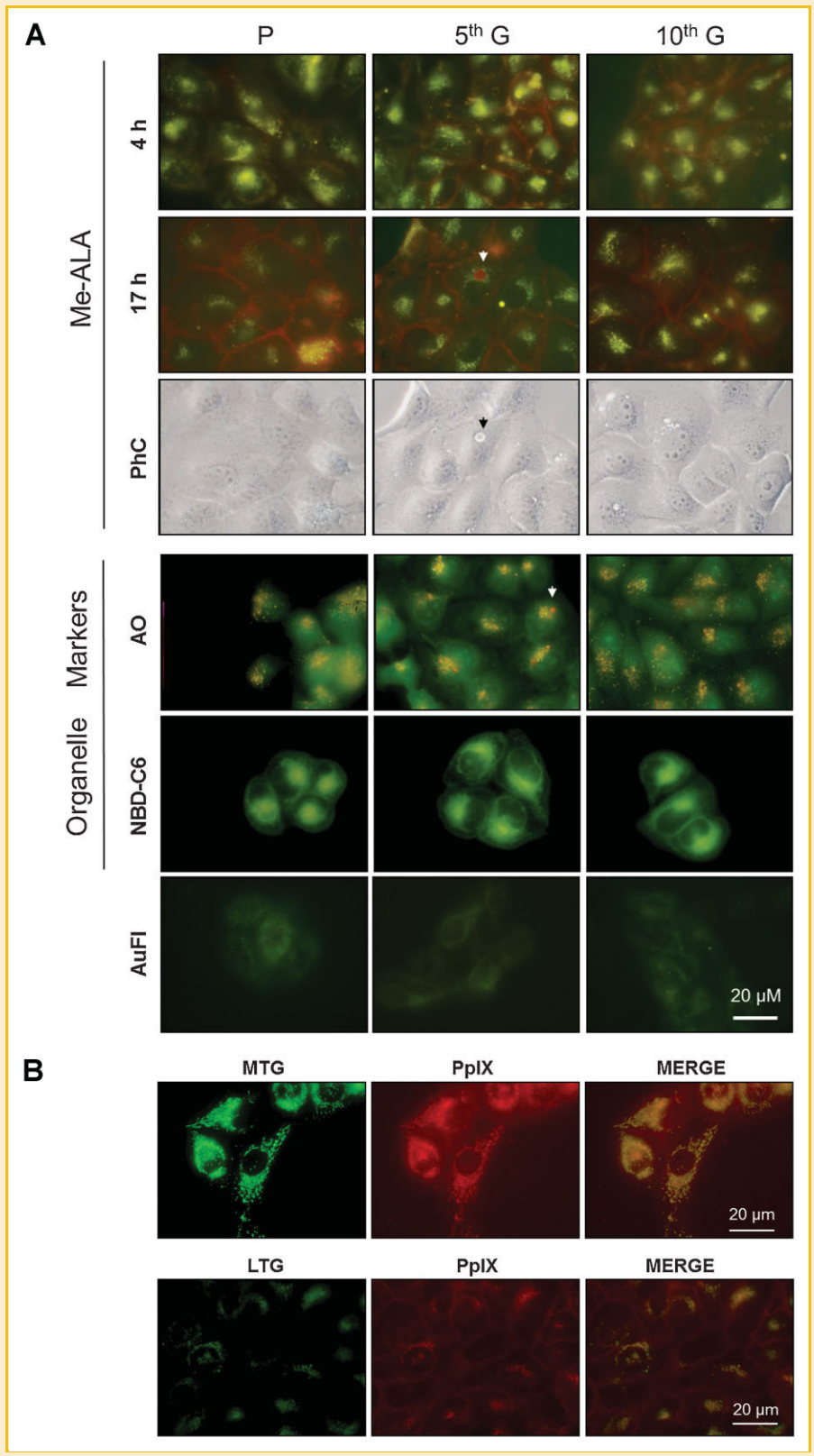

Fig. 3. PpIX localization in SCC cells. A: PpIX fluorescing in red under blue exciting light ($\lambda_{exc} = 460–490$ nm) after 4 and 17 h of incubation with 1 mM Me-ALA in SCC parental, 5th and 10th resistant generations. The patterns of organelles markers acridine orange (lysosomes) and NBD-C6 ceramide (Golgi apparatus) are shown. Arrows indicates vacuoles. G: generation. P: parental. B: Colocalization of PpIX and Mitotracker Green and Lisotracker Green in SCC cells. PhC: phase contrast; AO: acridine orange; NBD-C6: NBD-C6 ceramide; AuFl: autofluorescence; MTG: Mitotracker Green; LTG: Lisotracker Green. Scale bar: 20 μm.

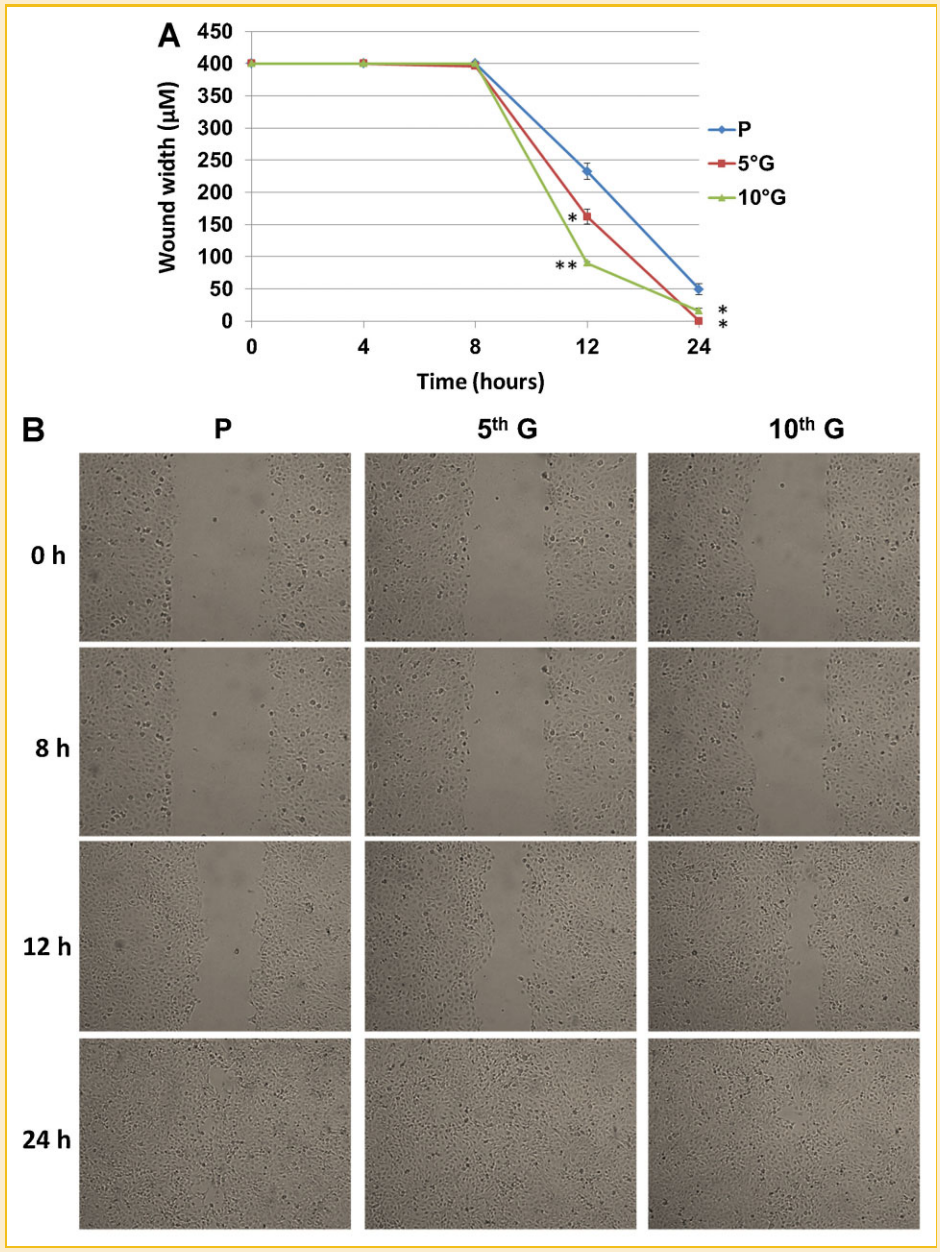

Fig. 4. Cell migration by scratch wound assay. A) The wound widths were measured in SCC-13 parental, 5th and 10th resistant generations at 4, 8, 12 and 24 h after the wounds were done. The values represent means ± standard errors. n = 8. * $P < 0.05$ (5th G-12 h vs P-12 h; 5th G-24 h vs P-24 h; 10th G-24 h vs P-24 h). ** $P < 0.01$ (10th G 12 h vs P 12 h). B) Photographs of the wounds in SCC-13 parental, 5th and 10th resistant generations at 0, 8, 12 and 24 h after the wounds were done. G: generation. P: parental.

resistant and parental cells (Fig. 5A and B). E-cadherin was localized in membrane, cytoplasm and nucleus, while β-catenin was mainly found in membrane and cytoplasm in all the analyzed cell populations.

CELL-SUBSTRATE ADHESION PROTEINS

Since we did not find differences in expression and distribution of cell-cell adhesion proteins, we next decided to evaluate the expression levels of cell-substrate adhesion proteins β1-integrin, vinculin, FAK and phospho-FAK by Western blot. Indirect immunofluorescence was employed to analyze the expression patterns of vinculin and phospho-FAK. In resistant cells vinculin and phospho-FAK showed a distribution in the center and in the borders of cells, while in parental cells the distribution was mainly in the borders (Fig. 6A). Vinculin was localized in the end of the stress fiber in the three studied populations (data not shown). SCC resistant cells of 5th and 10th generations had higher expression of β1-integrin, vinculin and phospho-FAK with respect to parental cells, whereas the levels of total FAK did not show differences between resistant and parental cells (Fig. 6B).

CYTOSKELETON PROTEINS

The cytoskeleton protein α-tubulin formed long filaments (microtubules) and dense nets in all the studied populations (Fig. 7). The

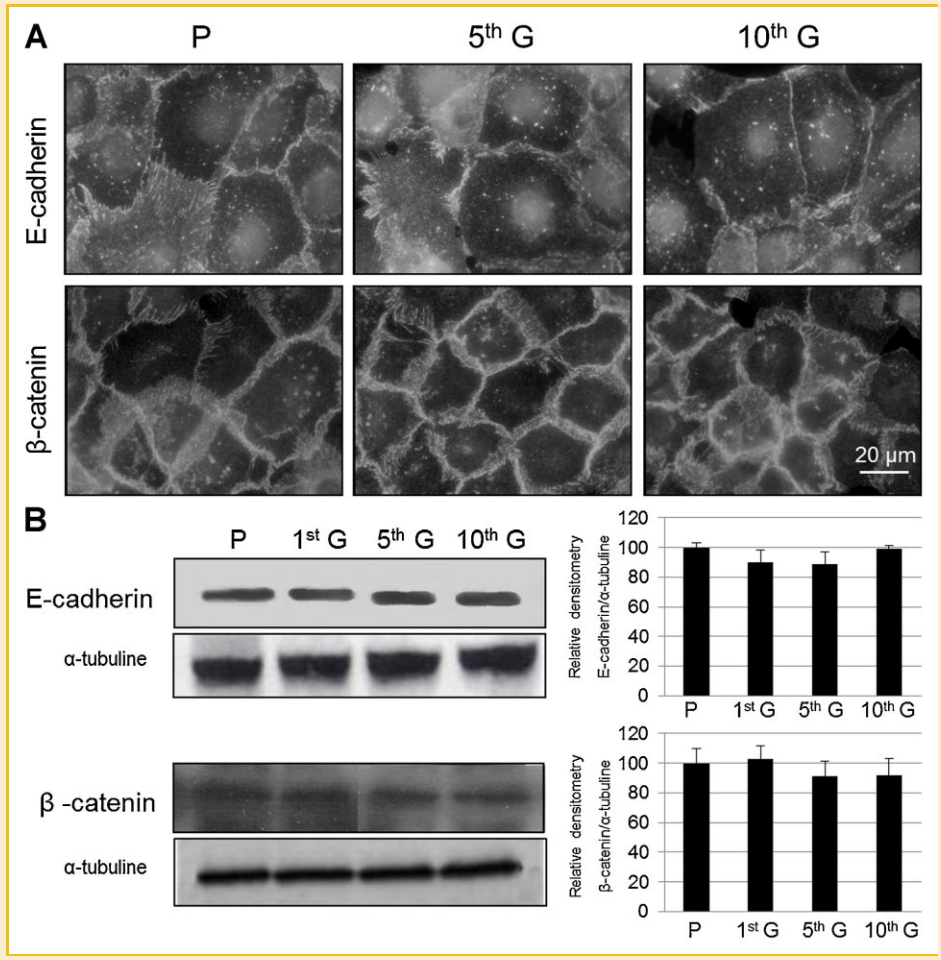

Fig. 5. Distribution patterns and expression levels of cell-cell adhesion proteins in SCC cells. A: Indirect immunofluorescence of E-cadherin and β-catenin in SCC-13 parental, 5th and 10th resistant generations. Scale bar: 20 μm. B: Western blot of E-cadherin and β-catenin in SCC-13 parental, 1st, 5th and 10th PDT-resistant generations. α-tubuline was used as proteins charge control. The values represent means ± standard errors. n = 3. G: generation. P: parental.

general organization of microtubules did not be substantially altered in resistant cells. In cells of fifth and tenth generations there were, however, a higher number of cells with long cytoplasm projections, accompanied of long filaments of α-tubulin, in respect to the parental cells.

Additionally, we next analyzed the pattern of the actin stress fibers of parental and PDT-resistant cells stained with rhodamine-phalloidin. Whereas in parental cells, F-actin was expressed mainly in cortical regions and showed stress fibers, in 5th and 10th resistant generations F-actin was highly expressed in cortical regions and many cells showed conspicuous stress fibers (Fig. 7). Furthermore, the stress fibers were more abundant in tenth generation than fifth generation. Convolved images of F-actin distribution confirmed the pattern indicated.

INHIBITOR OF APOPTOSIS PROTEIN

In order to better understand the mechanisms by which SCC are resistant to PDT treatment, we analyzed the expression pattern of a member of the inhibitor of apoptosis (IAP) family. Total survivin and phospho-survivin was localized in nucleus and cytoplasm in all the studied populations (Fig. 8A). The levels of total survivin did not show differences between resistant and parental cells. However, resistant cells had phospho-survivin expression levels markedly increased respect to parental cells and these levels were higher at the same time as resistance increased (Fig. 8B).

DISCUSSION

Many organelles can be affected by PDT, such as mitochondria, lysosome, nucleus, plasmatic membrane; also can be affected cell adhesion and cytoskeleton (microtubules, microfilaments and intermediate filaments) [Juarranz et al., 1995; Juarranz et al., 2001; Galaz et al., 2005]. The alteration of these structures activates a broad spectrum of signalization cascades, whose final balance led to tumor cell death. Nevertheless, one of the problems of PDT and of other cancer therapies is that resistant cells can arise [Perona and Sánchez-Pérez, 2004]. The inability of suffering apoptosis in response to the treatment offers a selective advantage in tumor progression and resistance to the therapies. In the present work, we

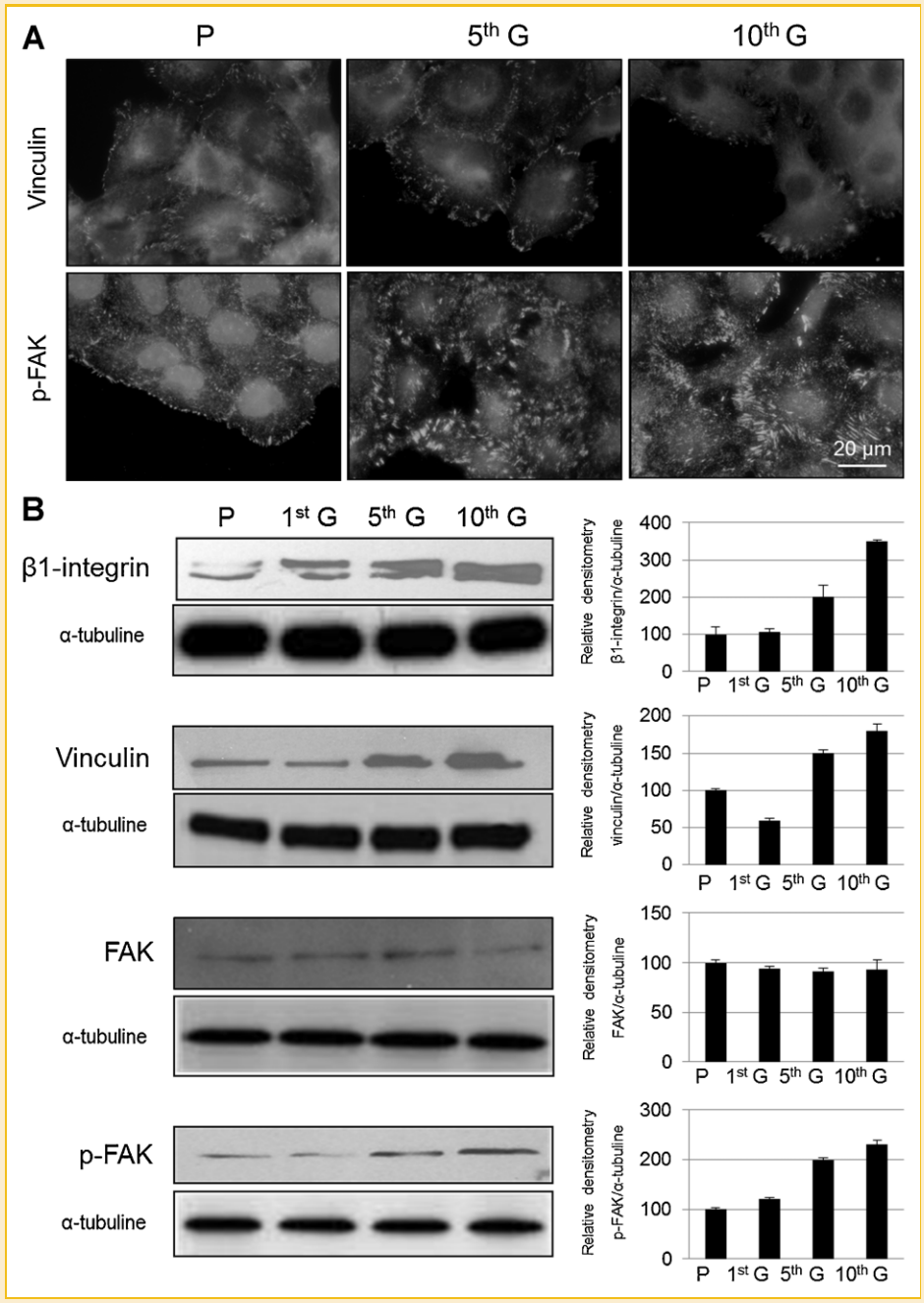

Fig. 6. Distribution patterns and expression levels of cell-substrate adhesion proteins in SCC cells. A: Indirect immunofluorescence of vinculin and p-FAK in SCC-13 parental, 5th and 10th resistant generations. Scale bar: 20 μm. B: Western blot of β1-integrin, vinculin, total FAK and phospho-FAK in SCC-13 parental, 1st, 5th and 10th PDT-resistant generations. α-tubuline was used as proteins charge control. The values represent means ± standard errors. n = 3. G: generation. G: generation. P: parental.

characterized squamous carcinoma cells SCC-13 resistant to Me-ALA-PDT.

Cells resistant to PDT have been obtained using exogenous photosensitizers, such as Photofrin and phthalocyanines [Singh et al., 2001] and the endogenous compound ALA [Casas et al., 2006]. Our results using Me-ALA showed that the PDT conditions must be more intensive to obtain the last SCC resistant generations and that resistant cells have a higher viability after PDT compared with parental cells. These would demonstrate a selection process of cells that, through some mechanisms, resist to PDT. We can hypothesized that from a heterogeneous group of initial cells, PDT would positively select those cells that posses resistant mechanisms, while cells that do not have these mechanisms die after treatment. On the other hand, it is tempting to speculate that the therapy would stimulate a higher expression of molecules that induce resistance.

We observed that resistant cells had a more fibroblastic morphology and a colony growth pattern more dendritic in respect to parental SCC. Our results of cell morphology coincided with that

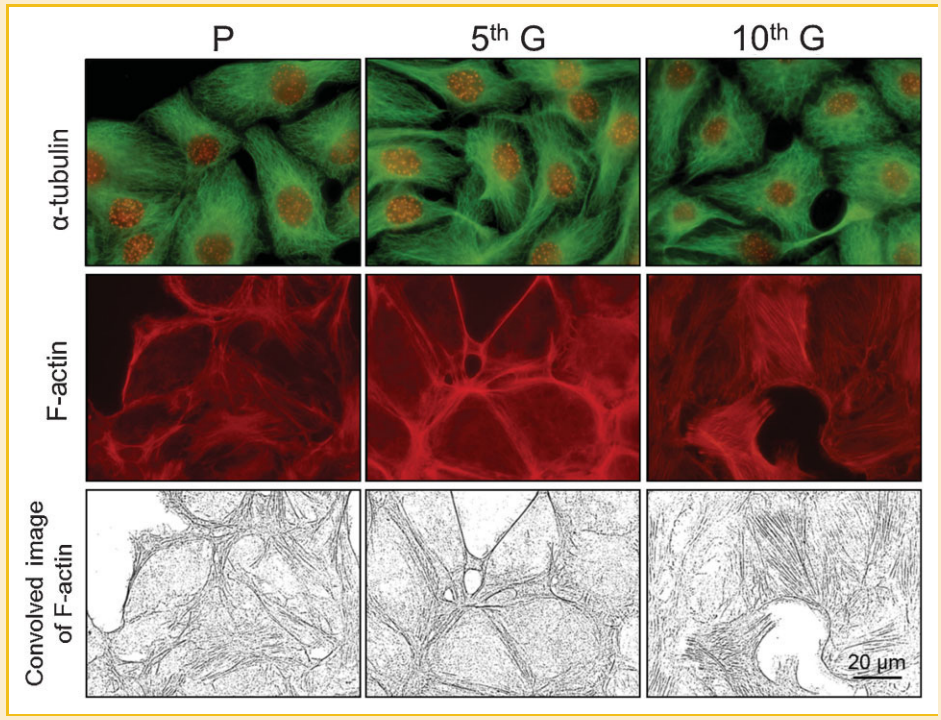

Fig. 7. Distribution patterns of the cytoskeleton proteins α-tubulin and F-actin. Cytoskeleton proteins were analyzed through indirect immunofluorescence (α-tubuline) and rhodamine-phalloidin stain (F-actin) in SCC-13 parental, 5th and 10th PDT-resistant populations. Convolved images of F-actin after white to black conversion are shown. G: generation. P: parental.

obtained in a study of ALA-PDT-resistant clones derived from the mammary adenocarcinoma LM3 line [Casas et al., 2006]. Considering the morphological characteristics of our SCC resistant cells, we can think that the resistant cells would have incremented migration ability. Differences were not founded in migration capacity between resistant and parental cells employing the scratch wound assay; however, SCC resistant cells might have an enhanced migration capacity on a tridimensional extracellular matrix.

In cancer cells, decrease in apoptosis mechanisms can be compensated by the process of mitotic catastrophe, resulting from abnormal mitosis and leading to the formation of cells with multiple micronuclei. The formation of micronuclei is studied to detect damage in vitro and in vivo after chemo- and radiotherapy in solid tumors with reduced apoptosis [Driessens et al., 2003]. There are not studies where the relationship between PDT resistance and the number of micronuclei is analyzed. Our PDT resistant cells have more number of micronuclei compared with parental cells, indicating disorganization in the genetic material in these malignant cells that have reduced cell death after PDT. The chromosomes from resistant cells that had not a correct separation during the anaphase might be forming the observed micronuclei. Although the genetic material migration during cell division is abnormal in some grade, this damage does not affect the viability of resistant cells, on the contrary the viability after PDT is increased in these cells and also some nucleuses are larger that parental cells, which would indicate a greater malignancy.

Since the cell phototoxicity might be affected by the amount of intracellular PpIX synthesized by the cells from ALA [Casas et al., 2006; Tsai et al., 2009] or Me-ALA, we examined if the differential cytotoxicity between parental and resistant cells was due to the different PpIX contents. There were not differences in PpIX fluorescence intensity, determinated by flow cytometry, between resistant and parental cells after 1 h of Me-ALA incubation. However, at 4 h after drug incubation lower fluorescence intensity of the photosensitizer was found in fifth generation resistant cells than in parental cells; therefore, we do not discard the idea that PDT-resistant SCC cells would have one or more mechanisms which allow accumulate lower intracellular PpIX amount. Multidrug resistant (MDR) family proteins are membrane ATPases that expulse a great variety of chemical compounds to the extracellular space avoiding their therapeutic action [Ullah, 2008]. The human MDR protein named ABCG2 o BCRP transports PpIX affecting the efficacy of PDT [Ishikawa et al., 2010]. Besides, resistant cells would have changes in the enzymatic system that regulates the synthesis of the PpIX from Me-ALA.

Although the absolute amount of intracellular PpIX plays the main determinant role for PDT effectivity, the intracellular localization pattern has additional effects on the mode of cell damage [Krieg et al., 2003; Ji et al., 2006]. Me-ALA induced PpIX was localized in the plasmatic membrane, cytoplasm, mitochondrias, and lysosomes in SCC resistant and parental cells. Moreover, in fifth generation cells PpIX was localized within big vacuoles. We can hypothesize that these vacuoles might be acting as sites of photosensitizer sequester. One resistant mechanism is the chemotherapeutic agents sequestration in acid vesicles, such as it happen with the doxorubicin in several cell lines which trap the drug

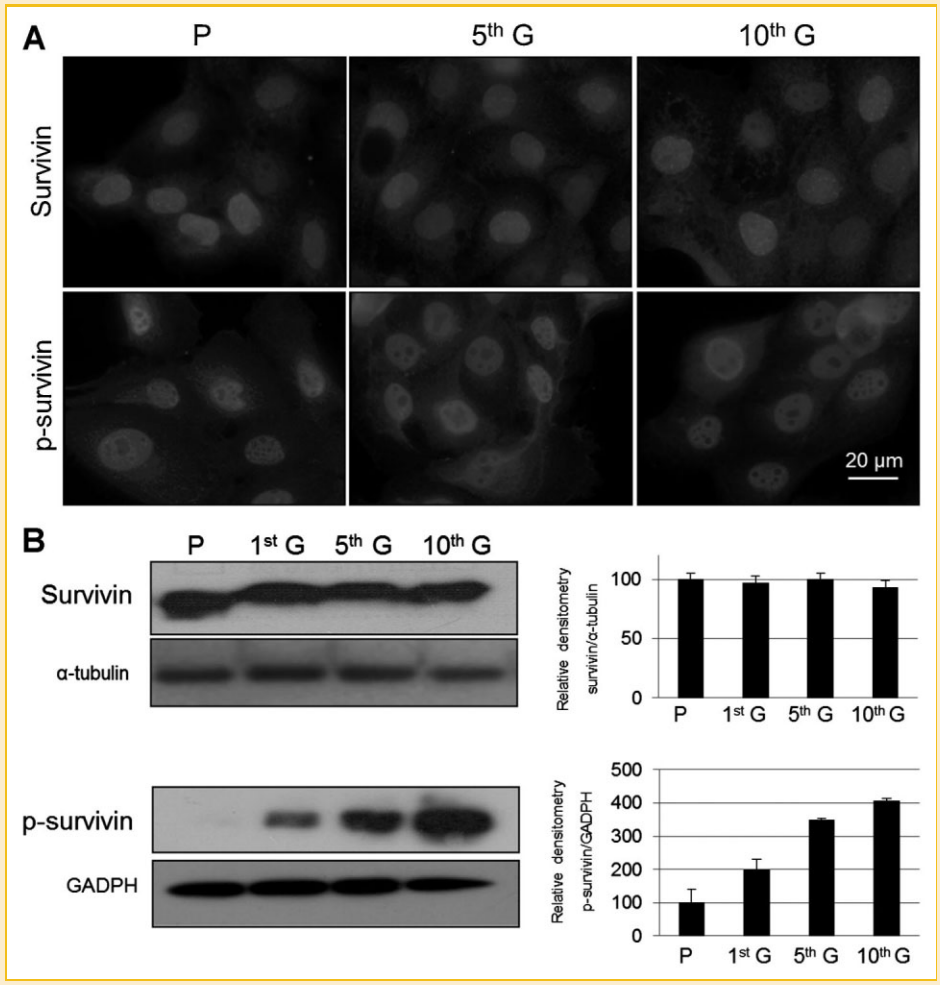

Fig. 8. Expression of the IAP survivin. A: Indirect immunofluorescence of total survivin and phospho-survivin in SCC-13 parental, 5th and 10th resistant generations. Scale bar: 20 μm. B: Western blot of total survivin and phospho-survivin in SCC-13 parental, 1st, 5th, and 10th PDT-resistant generations. GADPH was used as proteins charge control. The values represent means ± standard errors. n = 3. G: generation. P: parental.

in endocytic vesicles and exhibit a drug resistant phenotype [Ouar et al., 2003; Lou et al., 2006].

Different mechanisms can induce apoptosis including cell adhesion loss. Apoptosis relation with cell adhesion loss is named anoikis [Frisch and Francis, 1994]. In contrast, the increment in cell adhesion can induce chemo and radio-resistance [Hehlgans et al., 2007]. In our study it was observed that cell-cell adhesion proteins, E-cadherin and β-catenin, did not change their expression patterns and levels in resistant cells in respect to parental cells. Thus, we can conclude that the resistance was not granted by adherent junctions. Integrins family is currently the adhesion molecules group better documented by its role in cellular growth and survival [Hehlgans et al., 2007]. Many researchers demonstrated that integrins, mainly β1-integrins, of tumor cells cause resistance to different cytotoxic agents which have different action mechanisms [Hazlehurst and Dalton, 2001; Estrugo et al., 2007; Mori et al., 2008; Park et al., 2008]. In our investigation, cell-substrate adhesion proteins that constitute the focal adhesions, β1-integrin, vinculin and phospho-FAK, were increased in PDT-resistant cells. Also, in resistant generations conspicuous stress fibers were observed comparing with parental cells. The focal adhesion is a critical point for the regulation of actin organization [Ezzell et al., 1997; Defilippi et al., 1999; Zimerman et al., 2004]. In SCC-13 resistant cells we observed that vinculin was localized at the end of F-actin fibbers. From our results we can conclude that the resistance might be granted by focal adhesions.

While we did not found differences in the migration capacity between resistant and parental cells employing an assay in a bi-dimensional space, the scratch wound assay, we think that the increment in vinculin levels, β1-integrins and stress fibers in resistant cells might contribute to enhance their migration capacity in a tridimensional extracellular matrix. It was demonstrated that vinculin does not increases cell motility on a two-dimensional model, but facilitates three-dimensional matrix invasion by increasing transmission of traction forces that are needed to overcome the steric hindrance of the extracellular matrix [Mierke et al., 2010].

Survivin is an IAP that contributes to cancer progression and chemo-resistance and radio-resistance [Yamamoto et al., 2008]. It is expressed in basal cell carcinoma and in squamous cells carcinoma

and contributes to their progression [Grossman et al., 1999]. In our study, the active form of this IAP, phospho-survivin, was increased in resistant cell compared to parental cells, while total survivin levels were not altered. Me-ALA-PDT would induce the activation of survivin in SCC cells and this would be acting as a resistant mechanism to the treatment. It was observed that PDT increased the expression and phosphorylation of survivin in murine cancer cells and tumors and that the manipulation of the antiapoptotic pathway maintained by survivin may enhance PDT mediated cancer therapy [Ferrario et al., 2007]. Besides its function as inhibitor of apoptosis, survivin facilitates cell division [Yamamoto et al., 2008]. As it can been observed in the scratch wound assay, SCC-13 PDT-resistant cells had enhanced capacity of closing wounds probably because of higher proliferation, which would be related with an increment in the survivin activation or other proliferation proteins.

The findings of this report would be important to improve the efficacy and safety of PDT for squamous cell carcinoma. Currently, the functional relevance of the integrins pathway and survivin to the Me-ALA-PDT resistant phenotype of the squamous cell carcinoma is being studied in our laboratory.

ACKNOWLEDGMENTS

This research was supported by Agencia Española de Cooperación Internacional (AECI, A/010492/07), Consejo Nacional de Investigación Científica y Tecnológica (CONICET), Secretaría de Ciencia y Técnica (SeCyT) of Universidad Nacional de Río Cuarto (UNRC), PICT Agencia FONCYT and Ministerio de Ciencia e Innovación from Spain (FIS, PS09/0199). Authors thank Dr. Juan C. Stockert from Universidad Autónoma de Madrid and Mic. María Florencia Pansa from Universidad Nacional de Río Cuarto.

REFERENCES

Buño I, Juarranz A, Cañete M, Villanueva A, Gosálvez J, Stockert JC. 1998. Image processing and analysis of fluorescent labelled cytoskeleton. Micron 29:445–449.

Buytaert E, Dewaele M, Agostinis P. 2007. Molecular effectors of multiple cell death pathways initiated by photodynamic therapy. Biochem Biophys Acta 1776:86–107.

Casas A, Perotti C, Ortel B, Di Venosa G, Saccoliti M, Battle A, Hasan T. 2006. Tumor cell lines resistant to ALA-mediated photodynamic therapy and possible tools to target surviving cells. Int J Oncol 29:397–405.

Casas A, Sanz-Rodriguez F, Di Venosa G., et al. 2008. Disorganisation of cytoskeleton in cells resistant to photodynamic treatment with decreased metastatic phenotype. Cancer Lett 270:56–65.

Cordes N, Meineke V. 2003. Cell adhesion-mediated radioresistance (CAM-RR). Extracellular matrix-dependent improvement of cell survival in human tumor and normal cells in vitro. Strahlenther Onkol 179:337–344.

Defilippi P, Olivo C, Venturino M, Dolce L, Silengo L, Tarone G. 1999. Actin cytoskeleton organization in response to integrin-mediated adhesion. Microsc Res Tech 47:67–78.

Dougherty TJ, Gomer CJ, Henderson BW, Jori G, Kessel D, Korbelik M, Moan J, Peng Q. 1998. Photodynamic therapy. J Natl Cancer Inst 90:889–905.

Driessens G, Harsan L, Robaye B, Waroquier D, Browaeys P, Giannakopoulos X, Velu T, Bruyns C. 2003. Micronuclei to detect in vivo chemotherapy damage in a p53 mutated solid tumour. Br J Cancer 89:727–729.

Estrugo D, Fischer A, Hess F, Scherthan H, Belka C, Cordes N. 2007. Ligand bound beta1 integrins inhibit procaspase-8 for mediating cell adhesion-mediated drug and radiation resistance in human leukemia cells. PLos One 3:e269.

Ezzell RM, Goldmann WH, Wang N, Parasharama N, Ingber DE. 1997. Vinculin promotes cell spreading by mechanically coupling integrins to the cytoskeleton. Exp Cell Res 231:14–26.

Ferrario Á, Rucker N, Wong S, Luna M, Gomer CJ. 2007. Survivin, a member of the inhibitor of apoptosis family is induced by photodynamic therapy and is a target for improving treatment response. Cancer Res 67:4989–4995.

Frisch SM, Francis H. 1994. Disruption of epithelial cell-matrix interactions induces apoptosis. J Cell Biol; 124:619–626.

Galaz S, Espada J, Stockert JC, Pacheco M, Sanz-Rodriguez F, Arranz R, Rello S, Cañete M, Villanueva Á, Esteller M, Juarranz Á. 2005. Loss of E-cadherin mediated cell-cell adhesion as an early trigger of apoptosis induced by photodynamic treatment. J Cell Physiol 205:86–96.

Grossman D, McNiff JM, LI F, Altieri DC. 1999. Expression of the apoptosis inhibitor, survivin, in nonmelanoma skin cancer and gene targeting in a keratinocyte cell line. Lab Invest 79:1121–1126.

Hazlehurst LA, Dalton WS. 2001. Mechanisms associated with cell adhesion mediated drug resistance (CAM-DR) in hematopoietic malignancies. Cancer Metast Rev 20:43–50.

Hazlehurst L, Landowski T, Dalton W. 2003. Role of the tumor microenvironment in mediating de novo resistance to drugs and physiological mediators of cell death. Oncogene 22:7396–7402.

Hehlgans S, Haase M, Cordes N. 2007. Signalling via integrins: Implications for cell survival and anticancer strategies. Biochem Biophys Acta 1775:163–180.

Ishikawa T, Nakagawa H, Hagiya Y, Nonoguchi N, Miyatake S, Kuroiwa T. 2010. Key role of human ABC transporter ABCG2 in photodynamic therapy and photodynamic diagnosis. Adv Pharmacol Sci 2010:1–13.

Ji Z, Yang G, Vasovic V, Cunderlikova B, Suo Z, Nesland JM, Peng Q. 2006. Subcellular localization pattern of protoporphyrin IX is an important determinant for its photodynamic efficiency of human carcinoma and normal cell lines. J Photochem Photobiol 1:213–220.

Josefsen LB, Boyle RW. 2008. Photodynamic therapy and the development of metal-based photosensitisers. Met Based Drugs 2008:1–24.

Juarranz Á, Villanueva A, Díaz V, Cañete M. 1995. Photodynamic effects of the cationic porphyrin, mesotetra (4N-methylpyridyl) porphine, on microtubules of HeLa cells. J Photochem Photobiol B 27:47–53.

Juarranz Á, Espada J, Stockert JC, Villanueva Á, Polo S, Domínguez V, Cañete M. 2001. Photodamage induced by Zinc(II)-phthalocyanine to microtubules, actin, α-actinin and keratin of HeLa cells. J Photochem Photobiol B 73:283–289.

Kitano H. 2007. Cancer of a robust system: Implications for anticancer therapy. Nat Rev Cancer 4:227–235.

Krieg RC, Messmann H, Schlottmann K, Endlicher E, Seeger S, Schölmerich J, Knuechel R. 2003. Intracellular localization is a cofactor for the phototoxicity of protoporphyrin IX in the gastrointestinal tract: In vitro study. Photochem Photobiol 78:393–399.

Lou PJ, Lai PS, Shieh MJ, Macrobert AJ, Berg K, Bown SG. 2006. Reversal of doxorubicin resistance in breast cancer cells by photochemical internalization. Int J Cancer 119:2692–26928.

Luna M, Gomer C. 1991. Isolation and characterization of mouse tumor cells resistant to porphyrin-mediated photodynamic therapy. Cancer Res 51: 4243–4249.

Mierke CT, Kollmannsberger P, Paranhos Zitterbart D, Diez G, Koch TM, Marg S, Ziegler WH, Goldmann WH, Fabry B. 2010. Vinculin facilitates cell invasion into three-dimensional collagen matrices. J Cell Biol Chem 285: 13121–13130.

Mori R, Ishiguro H, Kuwabara Y, Kimura M, Mitsui A, Tomoda K, Mori Y, Ogawa R, Katada T, Harata K, Fujii Y. 2008. Targeting β1 integrin restores sensitivity to docetaxel of esophageal squamous cell carcinoma. Oncol Rep 20:1345–1351.

Ouar Z, Bens M, Vignes C, Paulais M, Pringel C, Fleury J, Cluzeaud F, Lacave R, Vandewalle A. 2003. Inhibitors of vacuolar H+-ATPase impair the preferential accumulation of daunomycin in lysosomes and reverse the resistance to anthracyclines in drug-resistant renal epithelial cells. Biochem J 370:185–193.

Park CC, Zhang HJ, Yao ES, Park CJ, Bissell MJ. 2008. Beta1 integrin inhibition dramatically enhances radiotherapy efficacy in human breast cancer xenografts. Cancer Res 68:4398–4405.

Perona R, Sánchez-Pérez I. 2004. Control of oncogenesis and cancer therapy resistance. Br J Cancer 90:573–577.

Rheinwald JG, Beckett MA. 1981. Tumorigenic keratinocyte lines requiring anchorage and fibroblast support cultured from human squamous cell carcinomas. Cancer Res 41:1657–1663.

Ricotti C, Bouzari N, Agadi A, Cockerell CJ. 2009. Malignant skin neoplasms. Med Clin North Am 93:1241–1264.

Rodel F, Hoffman J, Distel L. 2005. Survivin as a radioresistance factor and prognostic and therapeutic target for radiotherapy in rectal cancer. Cancer Res 65:4881–4887.

Rousset N, Vonarx V, Eléouet S., Carré J, Kerninon E, Lajat Y, Patrice T. 1999. Effects of photodynamic therapy on adhesion molecules and metastasis. J Photochem Photobiol B 52:65–73.

Seidler J, Durzok R, Brakebusch C, Cordes N. 2005. Interactions of the integrin subunit b1A with protein kinase B/Akt, p130Cas and paxillin contribute to regulation of radiation survival. Radiother Oncol 76:129–134.

Sieró A, Kawczyk-Krupka A, Wojciech Cebula MA, Szygula M, Zieleznik W, Gruk M, Suwala-Lurczyk B. 2004. Photodynamic therapy (PDT) using topically applied δ-aminolevulinic acid (ALA) for the treatment of malignant skin tumors. Photodiag Photodyn Ther 1:311–317.

Singh G, Espiritu M, Yun Shen X, Hanlon JG, Rainbow AJ. 2001. In vitro induction of PDT resistance in HT29, HT1376 and SK-N-MC cells by various photosensitizers. Photochem Photobiol 73:651–656.

Solyanik GI. 2010. Multifactorial nature of tumor drug resistance. Exp Oncol 32:181–185.

Szeimies RM. 2007. Methyl aminolevulinate photodynamic therapy for basal cell carcinoma. Dermatol Clin 25:89–94.

Szeimies RM, Morton CA, Sidoroff A, Braathen LR. 2005. Photodynamic therapy for nonmelanoma skin cancer. Acta Derm Venereol 85:483–490.

Tsai T, Tai Ji H, Chiang P, Chou R, Chang WW, Chen C. 2009. ALA-PDT results in phenotypic changes and decreased cellular invasion in surviving cancer cells. Lasers Surg Med 41:305–315.

Ullah MF. 2008. Cancer multidrug resistance: a major impediment to effective chemotherapy. Asian Pac J Cancer Prev 9:1–6.

Uzdensky AB, Juzeniene A, Kolpakova E, Hjortland GO, Juzenas P, Moan J. 2004. Photosensitization with protoporphyrin IX inhibits attachment of cancer cells to a substratum. Biochem Biophys Res Commun 322:452–457.

Velling T, Nilsson S, Stefansson A, Johansson S. 2004. Beta1-Integrins induce phosphorylation of Akt on serine 473 independently of focal adhesion kinase and Src family kinases. EMBO Rep 5:901–905.

Yamamoto H, Yee Ngan C, Monden M. 2008. Cancer cells survive with survivin. Cancer Sci 99:1709–1714.

Zaffaroni N, Pennati M, Colella G. 2002. Expression of the anti-apoptotic gene survivin correlates with taxol resistance in human ovarian cancer. Cell Mol Life Sci 59:1406–1412.

Zimerman B, Volberg T, Geiger B. 2004. Early molecular events in the assembly of the focal adhesion-stress fiber complex during fibroblast spreading. Cell Mot Cytosk 58:143–159.